Interface engineering of solution processed hybrid organohalide perovskite solar cells

Shanshan Zhang[1,2], Ardalan Armin[3], Qianqian Lin[4], Jan Sobus[1], Hellen Jin[1], Martin Stolterfoht[2], Paul L Burn[1], Paul Meredith[1,3], Dieter Neher[2]

1. Centre for Organic Photonics & Electronics (COPE), School of Chemistry and Molecular Biosciences and School of Mathematics and Physics, The University of Queensland, Brisbane 4072, Australia

2. Institute of Physics and Astronomy, University of Potsdam, Karl-Liebknecht-Str. 24-25, D-14476 Potsdam-Golm, Germany.

3. Department of Physics, Swansea University, Singleton Park, Swansea SA2 8PP Wales, United Kingdom

4. School of Physics and Technology, Wuhan University, Wuhan, 430072, P. R. China

Requests for materials and all correspondence should be addressed to:

neher@uni-potsdam.de; p.burn2@uq.edu.au;

Keywords: organohalide lead perovskites, solar cells, surface wetting, work function, oxygen plasma, transport layers

Abstract:

Engineering the interface between the perovskite absorber and the charge transporting layers has become an important method for improving the charge extraction and open-circuit voltage (V_{OC}) of hybrid perovskite solar cells. Conjugated polymers are particularly suited to form the hole-transporting layer, but their hydrophobicity renders it difficult to solution-process the perovskite absorber on top. Herein, oxygen plasma treatment is introduced as a simple means to change the surface energy and work function of "hydrophobic" polymer interlayers for the use as *p*-contacts in perovskite solar cells. We find that upon oxygen plasma treatment, the "hydrophobic" surfaces of different prototypical *p*-type polymers became sufficiently hydrophilic to enable subsequent perovskite junction processing. In addition, the oxygen plasma treatment also increased the ionisation potential of the polymer such that it became closer to the valance band energy of the perovskite. It was also found that the oxygen plasma treatment could increase the electrical conductivity of the *p*-type polymers, facilitating more efficient charge extraction. Based on this concept, inverted $MAPbI_3$ perovskite devices with different oxygen plasma treated polymers such as P3HT, P3OT, PolyTPD or PTAA were fabricated with power conversion efficiencies of up to 19%.

1. Introduction:

It has been 7 years since the first organic−inorganic hybrid lead-based perovskite solar cells (PSCs) were reported with a power conversion efficiency (PCE) of 3.8%.[1] Rapid development of the technology has now led to PSCs with certified efficiencies of 22.7%,[2] which already surpasses traditional thin film solar technologies on small-scale devices (< 1cm^2). Arguably, the key factor driving this development is the solution processability of the perovskite absorber, which allows relatively simple and potentially scalable solar cell fabrication. The current generation of state-of-the-art PSCs require selective charge transport layers (CTLs) adjacent to the perovskite absorber to efficiently extract photogenerated electrons and holes *via* their respective electrodes. However, the current CTLs limit the efficiency of PSCs below the thermodynamic potential due to their imperfect charge selectivity and their comparatively low mobilities, both of which cause additional interfacial non-radiative recombination and hence FF and voltage losses.[3–7]

The most common electron extraction layers employed to-date are titanium dioxide (TiO_2)[8,9] and tin(IV) oxide (SnO_2),[3] due to their near-ideal charge selectivity and comparatively high carrier mobilities.[10] These CTLs are used in the so-called conventional perovskite cell *nip* configuration where the perovskite layer is sandwiched between an electron/hole transport layer (ETL/HTL) at the bottom/top, respectively. However, concerns remain regarding the long-term stability of TiO_2 due to its photocatalytic properties when exposed to UV light.[11,12] The alternative inverted *pin*-cell structure possesses the advantage of a particularly simple architecture requiring only a few nm of hole and electron extraction (or inter-) layers that can be spin coated from solution without the need for high temperature treatments. Using such ultrathin CTLs also lifts the necessity for chemical doping,[4] which has been linked to accelerated device degradation, e.g., due to de-doping over time as well as inferior device reproducibility.[13,14]

With respect to the hole transporting layer there is a wide selection of suitable organic semiconductors available,[13] with common ones including non-polymeric molecular donors such as Spiro-OMeTAD [2,2′,7,7′-tetrakis(N,N-di-p-methoxyphenyl-amine)9,9′-spirobifluorene] and TAPC (4,4′-Cyclohexylidenebis [N,N-bis(4-methylphenyl) benzenamine]), and polymeric hole-transporters such as PEDOT:PSS [poly(3,4-ethylenedioxythiophene):poly(styrenesulfonate)], polyTPD [poly(*N*,*N*'-bis-4-butylphenyl-*N*,*N*'-bisphenyl) benzidine] or PTAA [poly(bis{4-phenyl}{2,4,6-trimethylphenyl}amine)]. In particular, polymers are currently attracting significant attention: for example PTAA is presently employed in the highest certified PSC devices in both *nip*[8] and *pin* configurations,[15] even outperforming

the omnipresent Spiro-OMeTAD. The use of conjugated polymers for PSCs benefits from the related scientific fields of organic electronics and organic photovoltaics. However, the hydrophobic nature of these conjugated polymers complicates the perovskite deposition from solution due to surface energy mismatch. In fact, in previous works the perovskite absorber had to be evaporated in order to fabricate a planar *pin*-type perovskite cells with a polymeric HTL as bottom layer.[16,17] Examples of such an approach include polyTPD,[18] DPP-DTT [poly(2,5-(2-di(thien-2-yl)-thieno[3,2-b]thiophene))], PCDTBT [poly(*N*-9'-heptadecanyl-2,7-carbazole-*alt*-5,5-(4',7'-di(thien-2-yl)-2',1',3'-benzothiadiazole))], and P3HT [poly(3-*n*-hexylthiophene)].[19] In an attempt to overcome the hydrophobicity issue, a thermal annealing-induced interdiffusion method was introduced by Bi et al. in 2015 for the deposition of the perovskite layer.[20] This enabled, for the first time, the direct deposition of a solution processed perovskite on top of several hydrophobic HTLs and it was shown that this approach resulted in high-aspect-ratio crystalline grain growth. However, the perovskite deposition method required 2-steps (the PbI_2 and MAI were deposited sequentially), which is generally more challenging to precisely control the perovskite stoichiometry. Very recently, in another attempt to overcome the hydrophilicity issue, an additional interface modifier, PFN [poly({9,9-bis[3′-(*N*,*N*-dimethylamino)propyl]-2,7-fluorene}-*alt*-2,7-{9,9-dioctylfluorene})] was introduced by Lee et al.,[21] with the amphiphilic properties of the PFN providing a link between the hydrophobic HTL and the hydrophilic ionic perovskite. While the proposed method allowed fabrication of uniform perovskite films, even for large area cells (> 1 cm^2), PFN represents an additional layer that further increases the complexity of the cell structure.

Motivated by these facts, here we describe a general approach for increasing the hydrophilicity of organic semiconductor HTLs while also increasing their ionization potential towards the perovskite valence band. In particular, we report a short (5s) oxygen plasma treatment to modify the surface energy and hydrophobicity of suitable polymeric hole transport layers. We demonstrate that this method allows direct spin-coating of the traditional perovskite methyl ammonium lead iodide MAPI onto organic semiconductors such as PTAA, PolyTPD, P3HT and P3OT which, notably, would not be easily achieved without the treatment. We present a detailed investigation of the chemical, morphological and energetic properties of the interlayers using Kelvin probe measurements and photoelectron spectroscopy. We demonstrate that the approach allows fabrication of high quality pin-hole free perovskite absorber layers, which facilitates high power conversion efficiencies of up to 19% with respectable reproducibility.

2. Results and Discussion

2.1. Effect of oxygen plasma treatment on perovskite film morphology

It is well known that the surface energy and the morphology of thin film hole transport layers are critical factors affecting the perovskite deposition and crystal formation. Both depend on several parameters such as chemical heterogeneities, surface roughness, and molecular rearrangement.[22] Therefore, in the first part of the study the effect of the oxygen plasma treatment on the surface energy of the HTLs was investigated using water contact angle measurements. **Figure 1** shows the contact angle of polymer films on glass that were exposed to an oxygen plasma for 5 seconds (right column) compared to as-deposited films without the treatment (left column). The left column [Figure 1(**a**), 1(**c**), 1(**e**) and 1(**f**)] demonstrates the hydrophobic nature of the as-deposited PolyTPD, PTAA, P3HT and P3OT films, respectively, which all have a contact angle greater than 90º. After the oxygen plasma treatment it can be clearly seen in Figure 1(**b**), 1(**d**), 1(**f**) and 1(**h**) that the surface energy has decreased resulting in contact angles of < 60°. As a side remark, we noted a decrease in the UV-Vis absorption indicating a reduction in the film thickness (~ 25%) or film density after the treatment. In addition, the plasma treated P3OT and P3HT films revealed a decrease in the intensity of the long wavelength shoulder of their main absorption band, indicating some reduction of the polymer aggregation in the layer. (**Supplementary Figure S1**). However, given that amorphous polymers are the most successful HTLs for PSCs we believe this is of minor importance. Moreover, a smaller thickness of the HTL can be beneficial for achieving high fill factors.[4] We also employed Atomic force microscopy (AFM) to study the surface roughness of different interlayers with and without the oxygen plasma treatment. From **Supplementary Figure S2** it can be seen that the surface roughness of the plasma treated films is essentially unchanged to the as-deposited films (the change in the root mean surface roughness is < 0.1 nm).

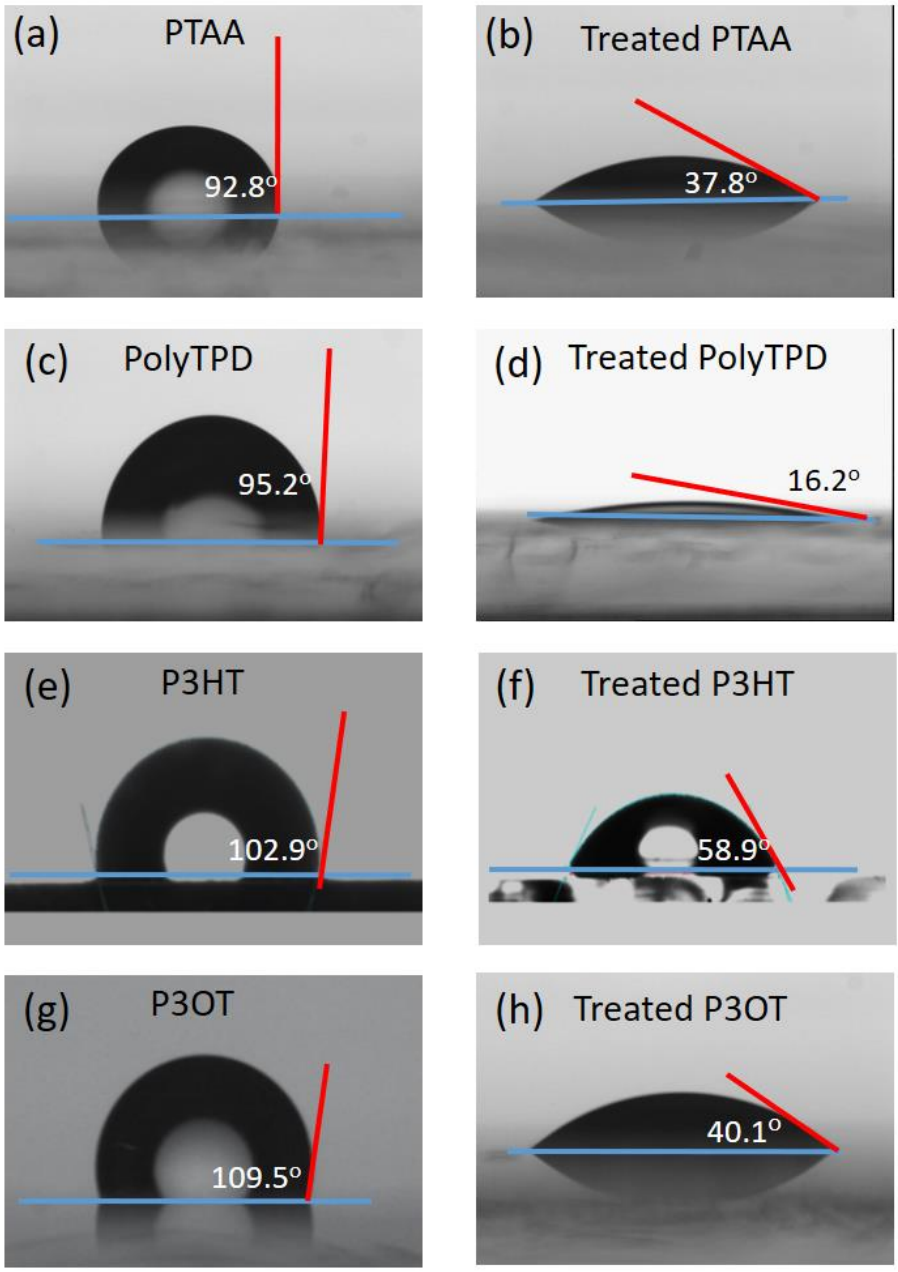

Figure 1. *Water contact angle of the p-type polymer films of interest: as-deposited (**a**) PolyTPD, (**c**) PTAA, (**e**) P3HT and (**g**) P3OT, and after 5 seconds oxygen plasma treatment (**b**) PolyTPD, (**d**) PTAA, (**f**) P3HT and (**h**) P3OT.*

The large decrease in the contact angle suggests an increased polarity of the polymer surface. In order to gain further insights into the surface chemistry of the oxygen plasma treated *p*-type interlayers X-ray photoeelectron spectroscopy (XPS) was performed. **Figure 2** shows the XPS spectra for P3HT and

PTAA respectively, while the results for P3OT and PolyTPD are shown in **Supplementary Figure S3**. In all cases, the signals corresponding to O 1s appear more strongly after oxygen plasma treatment of the film [Figures 2(**b**) and (**d**)]. **Supplementary Figure S4** (**a**) and (**b**) show that the O 1s peak of the P3HT film can be fitted with binding energies of 533.8 eV, 532.5 eV, 531.5 eV, and hence could correspond to O-C=O, O=C, O-C, and /or O-S respectively.[23,24] Similarly, the major fitted O 1s peak of the PTAA film at 532.5 nm corresponds to O=C bonds. Thus, we conclude that the surfaces of all films are oxidized through the oxygen plasma treatment, which we see as the main cause of the increased hydrophilicity (the contact angle decreases from 102.9° and 92.8° to 58.9° and 37.8° for the P3HT and PTAA films, respectively).

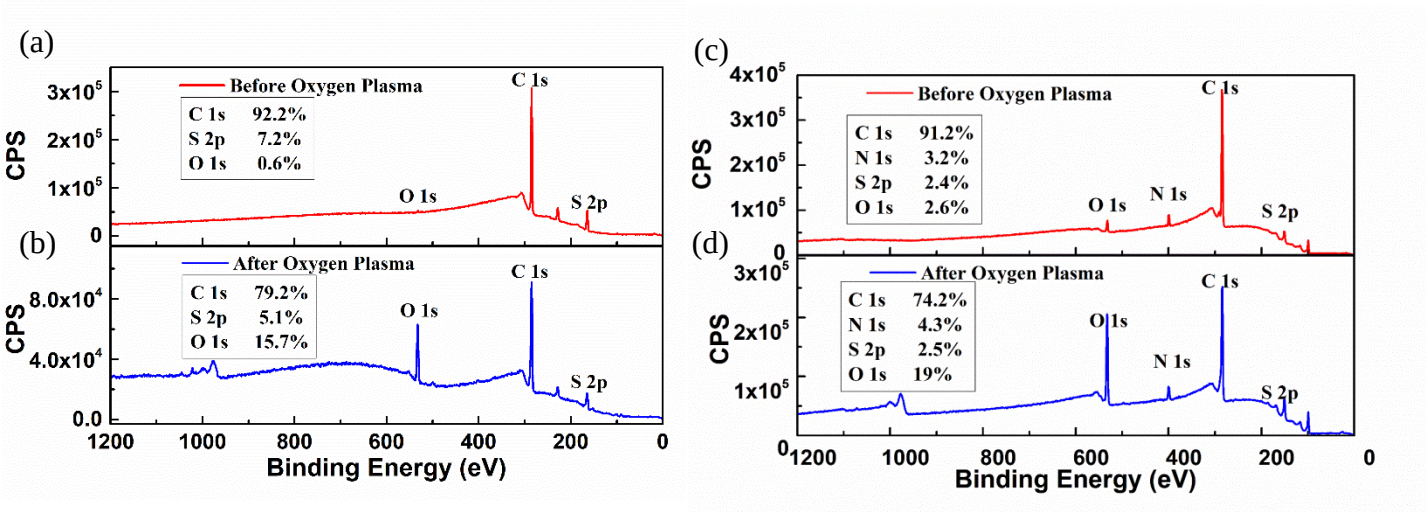

Figure 2. *X-ray photoelectron spectroscopy (XPS) measurements for neat (**a, c**) and oxygen plasma treated (**b, d**) P3HT and PTAA films, respectively. The oxygen (1s) signal of the neat films is around 3.4×10^3 and 6.0×10^3 counts, which increased to around 4×10^3 and 1.8×10^4 for the O_2 treated P3HT and PTAA films, respectively.*

2.2. Effect of oxygen plasma treatment on polymer layer energetics

It would be expected that the formation of an O-rich surface would alter the surface energetics of the layers. Thus, we performed Scanning Kelvin Probe Microscopy (SKPM) measurements on the polymer layers before and after the oxygen plasma treatment. An example of a SKPM measurement is shown in **Supplementary Figure S5**. The SKPM scans revealed a significant change of the work function upon plasma treatment, which is also highly across the surface. To obtain absolute values of the work function,

a standard highly oriented pyrolytic graphite (HOPG) sample (4.8 eV) was used as a reference, yielding a work function 5.3 eV for the tip. The contact potential difference = WF_{tip} - WF_{sample} was then measured for the PolyTPD, PTAA, P3HT, and P3OT films before and after plasma treatment, with the calculated relative work functions (WF) shown in **Table 1**. It can be seen that the WF increased considerably after the oxygen plasma treatment by 400 to 800 meV regardless of the polymer type. In order to correlate these results to changes in the energy levels itself, we also employed Photoelectron Spectroscopy in Air (PESA). The right column of **Table 1** shows that the IP increased for all four materials by approximately 200 – 500 meV upon the plasma treatment, moving the IP of the polymer layer closer to the valence band of the perovskite absorber of (5.5 eV), which is in principal beneficial for the open-circuit voltage.[5] Importantly, the increase of the ionization energy had a reasonable correlation with that of the untreated films. Thus, the combination of the XPS results and increased hydrophilicity leads to a surface layer with an increase in polarity and likely containing negatively charged oxygen-containing groups.

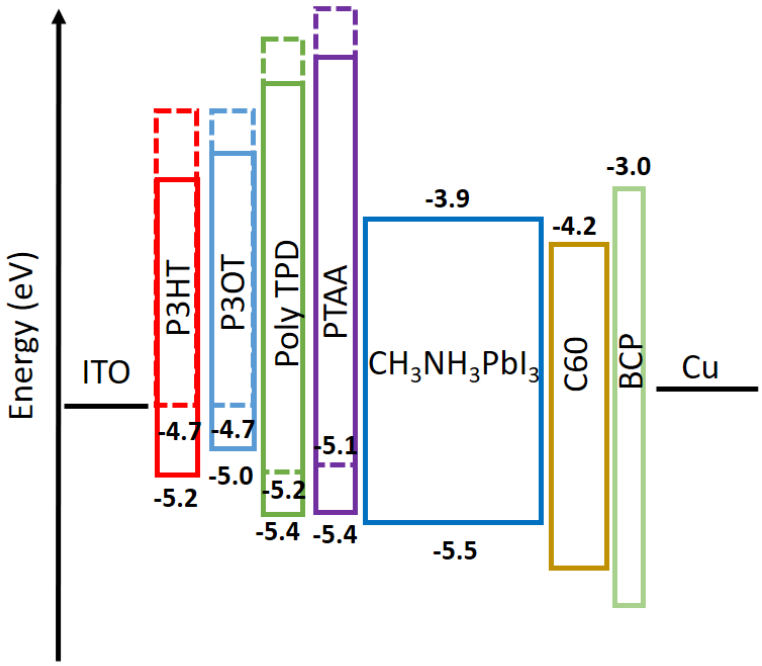

Figure 3. *Ionization energies (IEs) of the studied hole transporting materials (HTLs) measured using Photoelectron Spectroscopy in Air (PESA) before (dashed) and after the oxygen plasma treatment (solid lines) in addition to the energetics of the perovskite, the electrodes, and electron transport layers (ETLs). The energetics for the electrodes and ETLs were taken from literature, while the electron affinities of the HTLs and perovskite were determined from the IEs and the onset of the film absorption.*

	SKPM (Work function)				PESA (Ionization Potential)				
	P3HT	P3OT	Poly TPD	PTAA	P3HT	P3OT	Poly TPD	PTAA	$MAPbI_3$
Neat film	4.7eV	4.6eV	4.7eV	4.6eV	4.7eV	4.7eV	5.2eV	5.1eV	5.5eV
Treated film	5.1eV	5.2eV	5.4eV	5.3eV	5.2eV	5.0eV	5.4eV	5.4eV	

Table 1. *Change in work function and ionization potential (IP) of different polymer layers as measured by Kelvin Probe Microscopy and Photoelectron Spectroscopy in Air (PESA) before and after oxygen plasma treatment.*

The XPS measurements demonstrated the significant effect of the oxygen plasma treatment on the surface chemistry of the films. However, in addition the treatment could also lead to oxygen doping of the organic semiconductors. In particular, the effect of atmospheric oxygen on the conductivity and intrinsic carriers in P3HT films has been previously reported.[25,26] In order to check whether the conductivity increased upon the treatment we fabricated two terminal devices with electrodes of different channel widths evaporated onto the different polymer films, where the polymer thickness was around 10 nm to mimic that used in the complete devices. While, the conductivities of the amorphous polymers (PolyTPD, PTAA) were found to be below the detection limit of this approach ($< 10^{-8}$ S/cm) before and after treatment, for the poly(thiophenes) we observed a considerable increase in conductivity (from 10^{-7} S/cm and $8x10^{-5}$ S/cm to 10^{-6} S/cm and $3x10^{-4}$ S/cm for P3OT and P3HT, respectively) as shown in **Supplementary Figure S6**. This is consistent with oxygen doping of the thin polymer film surface upon the treatment.

Overall the above results demonstrate that oxygen plasma treatment renders the surface of various hole-transporting polymer layers hydrophilic, increases the work function and ionization energy of the layer, moving them closer to the perovskite valence band, and in the case of the poly(thiophenes) increased the electrical conductivity.

2.2 Inverted perovskite solar cells performance.

Motivated by these results, in the final part of the study we fabricated inverted perovskite solar cells of the architecture Glass/ITO/HTL*/Perovskite/C60/BCP/Cu using the plasma treatment HTL* with a thickness of approximately 10 nm. By employing the oxygen plasma treatment, smooth and uniform perovskite films could be formed by spin-coating from solution by a simple one-step deposition method (see **Supplementary Figure S7**). **Figure 4**(**a**) shows typical current density–voltage (*JV*) curves (under simulated one sun AM1.5G irradiation) of the optimized devices based on different *p*-type materials, and the averaged performance parameters for seven perovskite devices are summarized in **Table 2**. Both sets of cells with PTAA and P3HT had fill factors (FF) of up to 80% with average FFs above 78% and 77%, respectively. These high values indicate a low resistance between the ITO, the HTL, and the perovskite. Notably, the highest performance was obtained using a plasma treated PTAA layer as shown in **Figure 4**(**b**). This device achieved a PCE of 19% with a V_{oc} of 1.05 V, J_{sc} of 22.7 mA cm^{-2}, and FF of 80%, with negligible hysteresis. We also note that our devices containing the P3HT interlayer achieved the highest efficiency reported for an inverted P3HT containing perovskite device (with a PCE of 16% V_{oc} of 1.0 V, a J_{sc} of 20.1 mA cm^{-2}, and an FF of 80%). Cells containing PolyTPD achieved PCEs comparable to previous literature for *nip* cells,[27,28] while efficient cells containing P3OT as the HTL are not reported to our knowledge. Corresponding Incident Photon-to-Current Efficiency (IPCE) spectra are presented in **Supplementary Figure S8** (**a**) and (**b**) for devices with P3OT and PTAA, respectively. Lastly, we emphasize that it is not possible to fabricate these *pin*-cells without the oxygen plasma treatment of the HTL which explains the lack of reference solar cell performance data in **Table 2**.

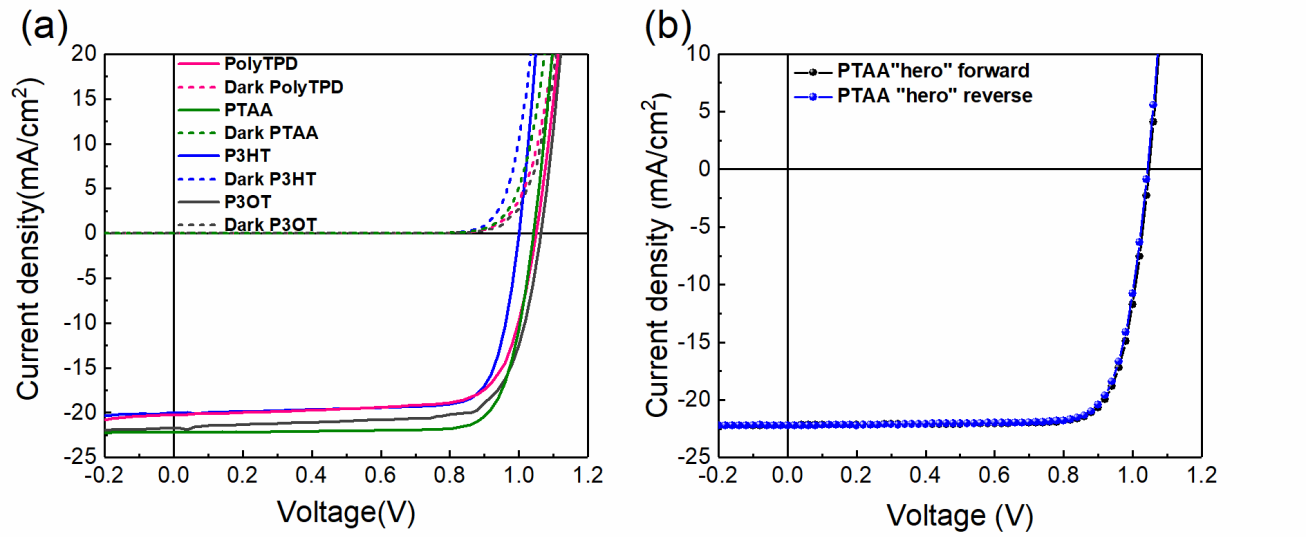

Figure 4. ***(a)*** *Dark and light J–V curves of the best performing plasma treated P3HT, P3OT, PolyTPD, PTAA interlayer* $CH_3NH_3PbI_3$ *perovskite solar cell* ***(b)*** *Light forward and reverse J–V curves (hysteresis measurement) of the "Hero" PTAA device.*

HTL	J_{sc} (mA/cm^2)	V_{oc} (V)	FF (%)	PCE (%) (Hero)
P3HT	20±0.3 (20.1)	1.00±0.01 (1.00)	0.79±0.01 (0.80)	16.0±0.1 (16.1)
P3OT	21±0.5 (21.7)	1.06±0.01 (1.06)	0.74±0.02 (0.75)	17.0±0.3 (17.4)
PolyTPD	20±0.3 (20.2)	1.05±0.01 (1.06)	0.75±0.01 (0.76)	16.0±0.1 (16.1)
PTAA	22±0.7 (22.7)	1.02±0.02 (1.05)	0.78±0.01 (0.80)	17.8±0.8 (19.0)

Table 2. *Photovoltaic performance parameters including the standard deviations and record parameters in brackets of inverted perovskite devices employing different interlayers under AM1.5G illumination (~100 mW cm*$^{-2}$*).*

3. Conclusions

In summary, we have shown that oxygen plasma treatment is a generic process to enable homogenous solution coating of an organohalide perovskite absorber onto conjugated *p*-type polymers. Oxygen plasma treatment results in a large increase of the surface energy, dramatically improving the wettability of the polymer layer with the polar perovskite solution. XPS measurements revealed the formation of an oxygen rich surface upon the plasma treatment leading to a substantial increase of both the work function and ionization potential, aligning the polymer energetics with the perovskite valence band. Conductivity measurements showed a conductivity increase of almost one order of magnitude for the oxygen plasma treated poly(thiophene) films, which minimized charge extraction losses. Finally, efficient perovskite solar cells were fabricated based on this method using different polymers as the hole transfer layers, with efficiencies reaching 19% for devices comprising an oxygen plasma treated PTAA HTL. We note that in the course of our work, UV-ozone treatment was recently proposed by Xu et al.[28] as an approach to modify the surface energy of common *p*-type polymers such as PolyTPD, and MEH-PPV. Our work complements these studies opening new possibilities to employ previously inapplicable hydrophobic polymeric hole transport layers for efficient planar inverted perovskite solar cells.

References:

(1) Kojima, A.; Teshima, K.; Shirai, Y.; Miyasaka, T. Organometal Halide Perovskites as Visible-Light Sensitizers for Photovoltaic Cells. *J. Am. Chem. Soc.* **2009**, *131* (17), 6050–6051.

(2) NREL. Best Research-Cell Efficiencies https://www.nrel.gov/pv/assets/images/efficiency-chart.png (accessed Dec 20, 2017).

(3) Correa-Baena, J.-P.; Tress, W.; Domanski, K.; Anaraki, E. H.; Turren-Cruz, S.-H.; Roose, B.; Boix, P. P.; Grätzel, M.; Saliba, M.; Abate, A.; et al. Identifying and Suppressing Interfacial Recombination to Achieve High Open-Circuit Voltage in Perovskite Solar Cells. *Energy Environ. Sci.* **2017**, *10* (5), 1207–1212.

(4) Stolterfoht, M.; Wolff, C. M.; Amir, Y.; Paulke, A.; Perdigón-Toro, L.; Caprioglio, P.; Neher, D. Approaching the Fill Factor Shockley–Queisser Limit in Stable, Dopant-Free Triple Cation Perovskite Solar Cells. *Energy Environ. Sci.* **2017**, *10* (6), 1530–1539.

(5) Wolff, C. M.; Zu, F.; Paulke, A.; Toro, L. P.; Koch, N.; Neher, D. Reduced Interface-Mediated Recombination for High Open-Circuit Voltages in CH3NH3PbI3 Solar Cells. *Adv. Mater.* **2017**, *29* (28), 1700159.

(6) Sherkar, T. S.; Momblona, C.; Gil-Escrig, L.; Bolink, H. J.; Koster, L. J. A. Improving Perovskite Solar Cells: Insights From a Validated Device Model. *Adv. Energy Mater.* **2017**, *7* (13), 1602432.

(7) Zheng, X.; Chen, B.; Dai, J.; Fang, Y.; Bai, Y.; Lin, Y.; Wei, H.; Zeng, X. C.; Huang, J. Defect Passivation in Hybrid Perovskite Solar Cells Using Quaternary Ammonium Halide Anions and Cations. *Nat. Energy* **2017**, *2* (7), 17102.

(8) Yang, W. S.; Park, B.; Jung, E. H.; Jeon, N. J.; Kim, Y. C.; Lee, D. U.; Shin, S. S.; Seo, J.; Kim, E. K.; Noh, J. H.; et al. Iodide Management in Formamidinium-Lead-Halide–based Perovskite Layers for Efficient Solar Cells. *Science* **2017**, *356* (6345), 1376–1379.

(9) Saliba, M.; Matsui, T.; Domanski, K.; Seo, J.-Y.; Ummadisingu, A.; Zakeeruddin, S. M.; Correa-Baena, J.-P.; Tress, W. R.; Abate, A.; Hagfeldt, A.; et al. Incorporation of Rubidium Cations into Perovskite Solar Cells Improves Photovoltaic Performance. *Science* **2016**, *354* (6309), 206.

(10) Tiwana, P.; Docampo, P.; Johnston, M. B.; Snaith, H. J.; Herz, L. M. Electron Mobility and

Injection Dynamics in Mesoporous ZnO, SnO 2, and TiO 2 Films Used in Dye-Sensitized Solar Cells. *ACS Nano* **2011**, *5* (6), 5158–5166.

(11) Leijtens, T.; Eperon, G. E.; Pathak, S.; Abate, A.; Lee, M. M.; Snaith, H. J. Overcoming Ultraviolet Light Instability of Sensitized TiO_2 with Meso-Superstructured Organometal Tri-Halide Perovskite Solar Cells. *Nat. Commun.* **2013**, *4*, 2885.

(12) Lee, S.-W.; Kim, S.; Bae, S.; Cho, K.; Chung, T.; Mundt, L. E.; Lee, S.; Park, S.; Park, H.; Schubert, M. C.; et al. UV Degradation and Recovery of Perovskite Solar Cells. *Sci. Rep.* **2016**, *6* (1), 38150.

(13) Calió, L.; Kazim, S.; Grätzel, M.; Ahmad, S. Hole-Transport Materials for Perovskite Solar Cells. *Angew. Chemie - Int. Ed.* **2016**, *55* (47), 14522–14545.

(14) Matsui, T.; Petrikyte, I.; Malinauskas, T.; Domanski, K.; Daskeviciene, M.; Steponaitis, M.; Gratia, P.; Tress, W.; Correa-Baena, J.-P.; Abate, A.; et al. Additive-Free Transparent Triarylamine-Based Polymeric Hole-Transport Materials for Stable Perovskite Solar Cells. *ChemSusChem* **2016**, *9* (18), 2567–2571.

(15) Zheng, X.; Chen, B.; Dai, J.; Fang, Y.; Bai, Y.; Lin, Y.; Wei, H.; Zeng, X. C.; Huang, J. Defect Passivation in Hybrid Perovskite Solar Cells Using Quaternary Ammonium Halide Anions and Cations. *Nat. Energy* **2017**, *2* (7), 17102.

(16) Lin, Q.; Armin, A.; Chandra, R.; Nagiri, R. R. C. R.; Burn, P. L.; Meredith, P. Electro-Optics of Perovskite Solar Cells. *Nat. Photonics* **2014**, *9* (2), 106.

(17) Polander, L. E.; Pahner, P.; Schwarze, M.; Saalfrank, M.; Koerner, C.; Leo, K. Hole-Transport Material Variation in Fully Vacuum Deposited Perovskite Solar Cells. *APL Mater.* **2014**, *2* (8), 81503.

(18) Tvingstedt, K.; Gil-Escrig, L.; Momblona, C.; Rieder, P.; Kiermasch, D.; Sessolo, M.; Baumann, A.; Bolink, H. J.; Dyakonov, V. Removing Leakage and Surface Recombination in Planar Perovskite Solar Cells. *ACS Energy Lett.* **2017**, *2* (2), 424–430.

(19) Lin, Q.; Armin, A.; Chandra, R.; Nagiri, R. R. C. R.; Burn, P. L.; Meredith, P. Electro-Optics of Perovskite Solar Cells. *Nat. Photonics* **2014**, *9* (2), 106.

(20) Bi, C.; Wang, Q.; Shao, Y.; Yuan, Y.; Xiao, Z.; Huang, J. Non-Wetting Surface-Driven High-Aspect-Ratio Crystalline Grain Growth for Efficient Hybrid Perovskite Solar Cells. *Nat. Commun.* **2015**, *6*, 1–7.

(21) Lee, J.; Kang, H.; Kim, G.; Back, H.; Kim, J.; Hong, S.; Park, B.; Lee, E.; Lee, K. Achieving Large-Area Planar Perovskite Solar Cells by Introducing an Interfacial Compatibilizer. *Adv. Mater.* **2017**, *29* (22), 1606363.

(22) Duc, C.; Vlandas, A.; Malliaras, G. G.; Senez, V. Wettability of PEDOT:PSS Films. *Soft Matter* **2016**, *12* (23), 5146–5153.

(23) Raj, K. J. A.; Shanmugam, R.; Mahalakshmi, R.; Viswanathan, B. XPS and IR Spectral Studies on the Structure of Phosphate and Sulphate Modified Titania - A Combined DFT and Experimental Study. *Indian J. Chem. - Sect. A Inorganic, Phys. Theor. Anal. Chem.* **2010**, *49* (1), 9–17.

(24) Shao, Y.; Zhang, S.; Engelhard, M. H.; Li, G.; Shao, G.; Wang, Y.; Liu, J.; Aksay, I. A.; Lin, Y. Nitrogen-Doped Graphene and Its Electrochemical Applications. *J. Mater. Chem.* **2010**, *20* (35), 7491.

(25) Liao, H. H.; Yang, C. M.; Liu, C. C.; Horng, S. F.; Meng, H. F.; Shy, J. T. Dynamics and Reversibility of Oxygen Doping and de-Doping for Conjugated Polymer. *J. Appl. Phys.* **2008**, *103* (10), 1–8.

(26) Hintz, H.; Peisert, H.; Egelhaaf, H. J.; Chasse, T. Reversible and Irreversible Light-Induced P-Doping of p3ht by Oxygen Studied by Photoelectron Spectroscopy (XPS/UPS). *J. Phys. Chem. C* **2011**, *115* (27), 13373–13376.

(27) Zhao, D.; Sexton, M.; Park, H. Y.; Baure, G.; Nino, J. C.; So, F. High-Efficiency Solution-Processed Planar Perovskite Solar Cells with a Polymer Hole Transport Layer. *Adv. Energy Mater.* **2015**, *5* (6), 1–5.

(28) Xu, X.; Ma, C.; Cheng, Y.; Xie, Y. M.; Yi, X.; Gautam, B.; Chen, S.; Li, H. W.; Lee, C. S.; So, F.; et al. Ultraviolet-Ozone Surface Modification for Non-Wetting Hole Transport Materials Based Inverted Planar Perovskite Solar Cells with Efficiency Exceeding 18%. *J. Power Sources* **2017**, *360*, 157–165.

Supporting Information

The Supporting Information is available on the ACS Applied Materials and Interfaces website.

Acknowledgements

The work was carried at the Centre for Organic Photonics & Electronics at The University of Queensland and the Institute of Physics and Astronomy, University of Potsdam. PLB is an Australian Research Council Laureate Fellow (FL160100067), PM a Sêr Cymru II Research Chair and AA a Sêr Cymru II Rising Star Fellow both at Swansea University. S.Z is funded by a Chinese Scholarship Council studentship. This work was performed in part at the Queensland node of the Australian National Fabrication Facility (ANFF-Q): a company established under the National Collaborative Research Infrastructure Strategy to provide nano and micro fabrication facilities for Australia's researchers. The authors acknowledge the facilities, the scientific and technical assistance of the Australian Microscopy & Microanalysis Research Facility at the Centre for Microscopy and Microanalysis, The University of Queensland. This Program has also been supported by the Australian Government through the Australian Renewable Energy Agency (ARENA) Australian Centre for Advanced Photovoltaics. Responsibility for the views, information, or advice expressed herein is not accepted by the Australian Government. Further support came from HyPerCells, a joint graduate school of the University of Potsdam and the Helmholtz Center Berlin. We finally thank the Fraunhofer-Institut für Angewandte Polymerforschung (IAP) for access to their PESA measurement setup.

Supplementary Information

Interface engineering of solution processed hybrid organohalide perovskite solar cells

Shanshan Zhang[1,2], Ardalan Armin[1,3], Qianqian Lin[1,4], Jan Sobus[1], Hellen Jin[1], Martin Stolterfoht[2], Paul L Burn[1], Paul Meredith[1,3], Dieter Neher[2]

1. Centre for Organic Photonics & Electronics (COPE), Chemistry and Molecular Biosciences and School of Mathematics and Physics, The University of Queensland, Brisbane 4072, Australia

2. Institute of Physics and Astronomy, University of Potsdam, Karl-Liebknecht-Str. 24-25, D-14476 Potsdam-Golm, Germany.

3. Department of Physics, Swansea University, Singleton Park, Swansea SA2 8PP Wales, United Kingdom

4. School of Physics and Technology, Wuhan University, Wuhan, 430072, P. R. China

Requests for materials and all correspondence should be addressed to:

neher@uni-potsdam.de; p.burn2@uq.edu.au;

Contents:

1. Experimental details:

1.1 Materials

Lead iodide (PbI_2, beads, 99 % trace metals basis), methylammonium iodide（MAI, 98%）were purchased from Alfa Aesar and Sigma-Aldrich. Poly[*N*-9'-heptadecanyl-2,7-carbazole-*alt*-5,5-(4',7'-di-2-thienyl-2',1',3'-benzothiadiazole)] (PCDTBT Mw = 122 kDa, polydispersity index (PDI) = 5.4) was purchased from SJPC, Canada. Fullerene-C60 (99.5%) was purchased from MTR Ltd. Poly(3-*n*-hexylthiophene) (P3HT, Mw = 52 kDa) was purchased from Merck. Poly(3-*n*-hexylthiophene) (P3HT, Mw = 145 kDa) was purchased from Merck. PTAA and BCP (Bathocuproine) were purchased from Sigma-Aldrich and Poly TPD from Ossila. All commercial products were used as received. The desired solutions of $CH_3NH_3PbI_3$ was prepared by dissolution of the MAI powder with PbI_2 in a γ-butyrolactone:DMSO mixed solvent (1.3 M, 7:3 by volume) at 60 °C for 10 min.[S1]

1.2 Oxygen plasma treatment

A Harrick oxygen plasma cleaner was used to treat the polymer films. The radio frequency (RF) level was turned to medium and pressure was kept at 53.33 pascals. All treatments were performed for 5 seconds.

1.3 Solar cells device fabrication

The solar cells were fabricated in a class 1000 clean room on commercial indium tin oxide (ITO) patterned glass electrodes (15 W/sq, Kintec). All the electrodes were cleaned in an Alconox (detergent) solution bath at 70 °C, followed by sonication in sequence with Alconox, Milli-Q water, acetone and 2-propanol for 10 min each. The cleaned substrates were dried with a stream of nitrogen and were transferred into a nitrogen glove box (O_2 <1 ppm, H_2O <1 ppm) for coating with 10±5 nm PTAA (2.5 mg/mL in toluene), PolyTPD (1.8mg/ml in chlorobenzene), P3OT and P3HT (3 mg/mL in *o*-dichlorobenzene) by spin-coating at 4000, 3000 rpm for 35 s, respectively. The substrates were transferred out of the glovebox for the 5 s oxygen plasma, and then transferred back into the glovebox for device fabrication. $CH_3NH_3PbI_3$ perovskite layers were then deposited via one step toluene assisted solution process. 80 μL of the perovskite solution was added on the top of oxygen plasma treated interlayer and spin-coated at 1000 rpm for 5 s and then 3000 rpm for 80 s. 100 μL of toluene was added

dropwise at 40 s to form a transparent perovskite film. After 5 minutes of annealing at 100 °C on a hot plate, the desired films with thickness of 350nm were obtained.[S2] After depositing the perovskite layer, 30 nm C60 and 8 nm BCP were evaporated on the top of perovskite, and finally 80 nm Cu was deposited by thermal evaporation under 10^{-6} mbar vacuum with an appropriate mask (6 mm^2 for each device), which defined the cell area, to complete the device.

1.4 Characterization

The absorption spectra of the films were measured using a Cary 5000 UV-Vis-NIR Spectrophotometer. The thickness and surface morphology were measured using a Veeco Dektak 150 and Cypher Atomic Force Microscopy (AFM), respectively. The work functions of films were measured using a Scanning Kelvin Probe Force Microscope (SKPM). The contact angle of polymer thin films were measured using a PSS OCA20 optical contact-measuring system. XPS measurements were undertaken on a Kratos Axis Ultra photoelectron spectrometer with mono Al Kα (1486.6eV) x-rays. Ionization potentials (HOMOs) of polymer interlayer films were measured at the Fraunhofer-Institut für Angewandte Polymerforschung IAP by Photoelectron Spectroscopy in Air (PESA).

1.5 Solar cell device performance measurement

J-V curves were obtained in a 2-wire source-sense configuration with a Keithley 2400. A filtered Oriel class AAA Xenon lamp was used for illumination providing approximately 100 mW cm^{-2} of AM1.5G irradiation and the intensity was monitored simultaneously with a Si photodiode. The exact illumination intensity was used for efficiency calculations, and the simulator was calibrated with a KG5 filtered silicon solar cell (certified by the Fraunhofer ISE). A spectral mismatch calculation was performed based on the spectral irradiance of the solar simulator, the EQE of the reference silicon solar cell and 3 typical EQEs of our cells. This resulted in 3 mismatch factors of M = 0.9949, 0.9996 and 0.9976. Given the very small deviation from unity the measured J_{SC} was not corrected by the factor $1/M$. The EQE spectrum was recorded with a (Philips Projection Lamp Type7724 12 V 100 W) in front of a monochromotor (Oriel Cornerstone 74100) and the light was mechanically chopped at 40 Hz. The photogenerated current was measured with a lock-in-amplifier (EG&G Princeton Applied Research Model 5302, integration times 300 ms-10 s) and evaluated after calibrating the lamp spectrum with an UV-enhanced Si photodetector (Newport).

Reference:

[S1] Jeon, N. J.; Noh, J. H.; Yang, W. S.; Kim, Y. C.; Ryu, S.; Seo, J.; Seok, S. I., *Nature* **2015,** *517* (7535), 476.

[S2] Lin, Q.; Stoltzfus, D. M.; Armin, A.; Burn, P. L.; Meredith, P., *Adv. Mater. Interfaces* **2016,** *3* (2), 1500420.

2. Supporting figures:

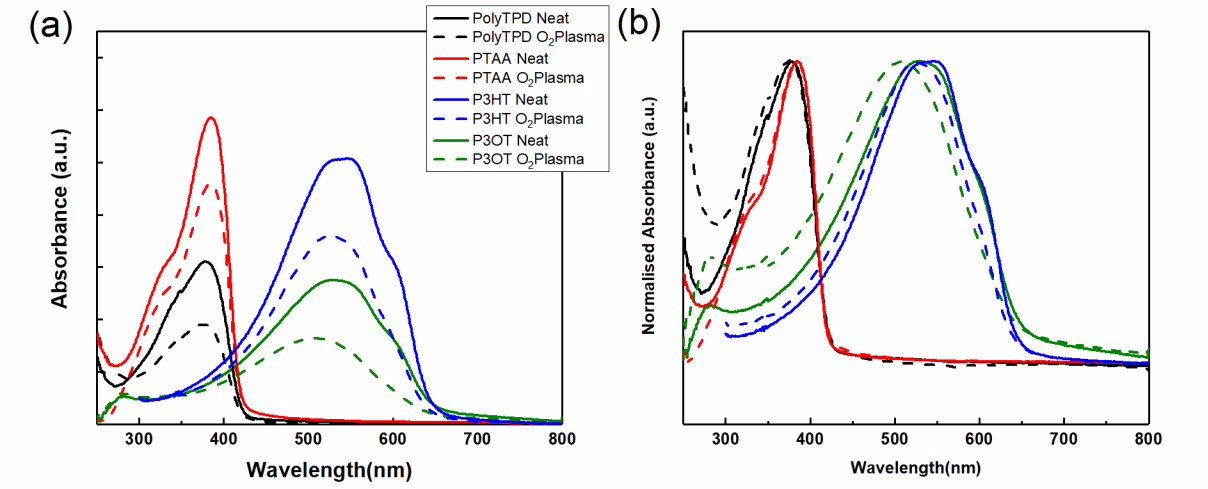

Supplementary Figure S1. *Original and peak normalized UV-vis spectra of different polymers used as interlayers before and after the oxygen plasma treatment of 5 seconds.*

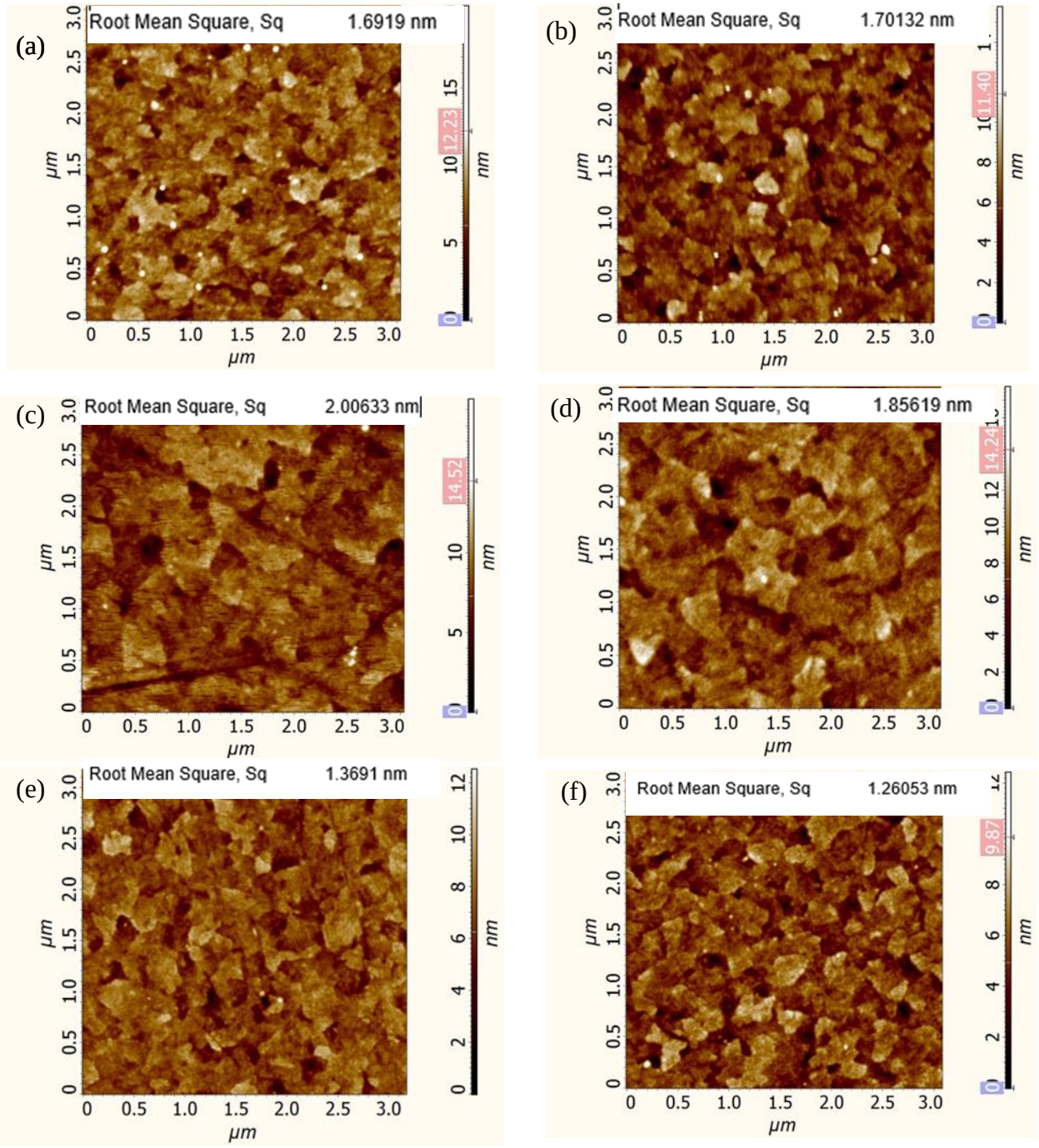

Supplementary Figure S2. *Atomic Force Microcopy (AFM) images (3 × 3 µm) of PolyTPD, P3OT and PTAA films before and after plasma treatment. Topography of a PolyTPD neat film before (a) and after plasma treatment (b); P3OT neat film before (c) and after plasma treatment (d); PTAA neat film before (e) and after plasma treatment (f). The bars next to the individual panels represent the height profile of*

the scanned area. The similar root mean square surface roughness demonstrates that the oxygen plasma treatment did not alter the roughness within the measurement error.

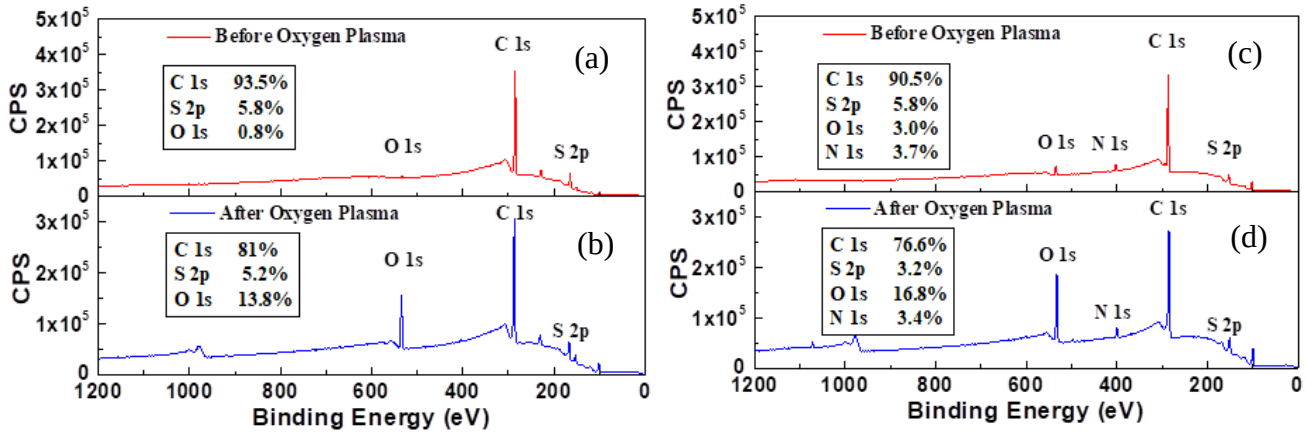

Supplementary Figure S3. *X-ray Photoelectron Spectroscopy (XPS) spectra of P3OT films (a) before and (b) after 5 seconds oxygen plasma treatment; PolyTPD films (c) before and (d) after 5 seconds oxygen plasma treatment*

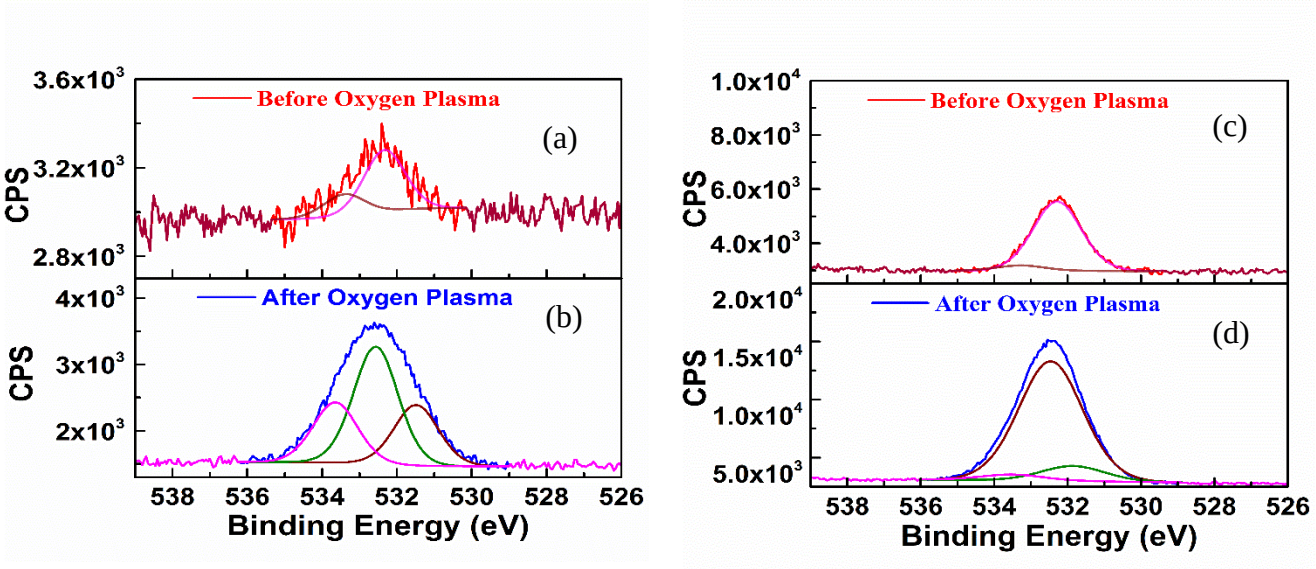

Supplementary Figure S4. *(a, b) XPS spectra of the O1s region for a neat and O_2 plasma treated P3HT film, respectively; similarly, (c, d) show the XPS spectra of the O1s region for a neat and O_2 plasma*

treated PTAA film, respectively. Also shown are Gaussian fits at different bindings energies which indicate O-C=O, O=C, O-C, and /or O-S bonds for the P3HT film, and O=C for the PTAA film.

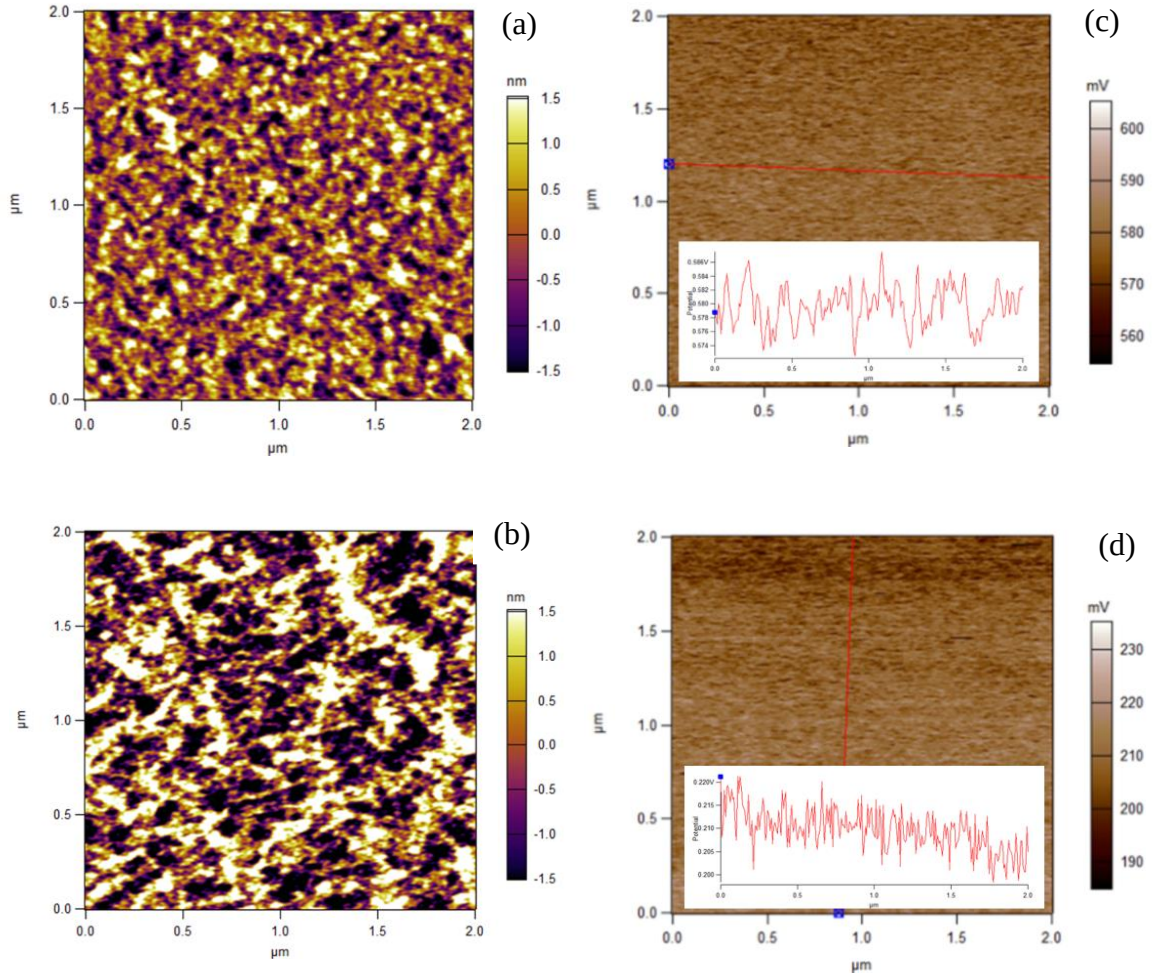

Supplementary Figure S5. *AFM and Scanning Kelvin Probe Microscopy (SKPM) images (2 × 2 µm) of P3HT films. Topography of a P3HT neat film before (a) and after P3HT plasma treatment (b). SKPM image of a P3HT neat film before (c) and after plasma treatment (d). The insets in (c) and (d) are the line sections over the corresponding films.*

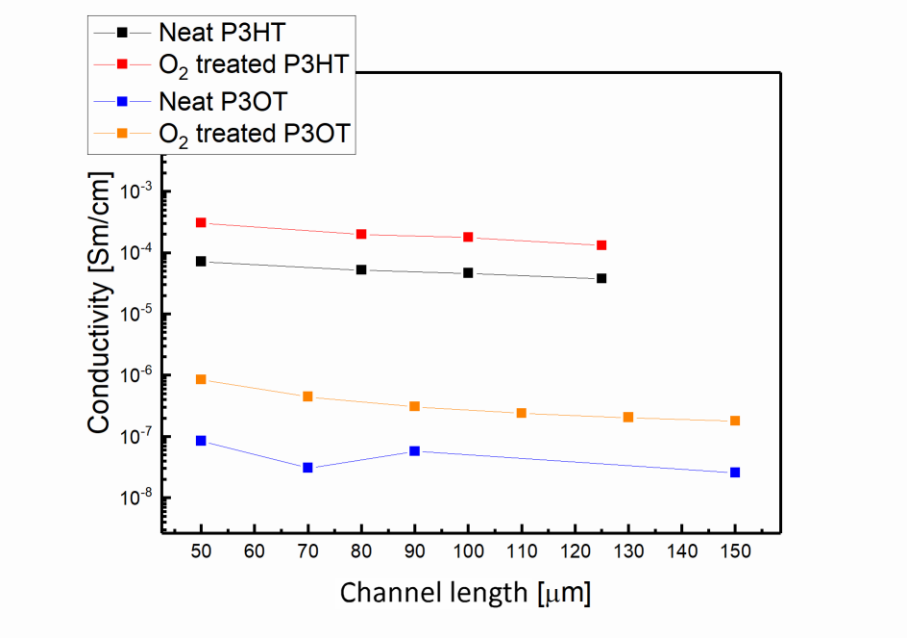

Supplementary Figure S6. *The electrical conductivity of poly(thiophene) HTLs as a function of channel width showing an increase upon the oxygen plasma treatment by 1 order of magnitude.*

Supplementary Figure S7. *Perovskite films deposited on PTAA with and without plasma treatment.*

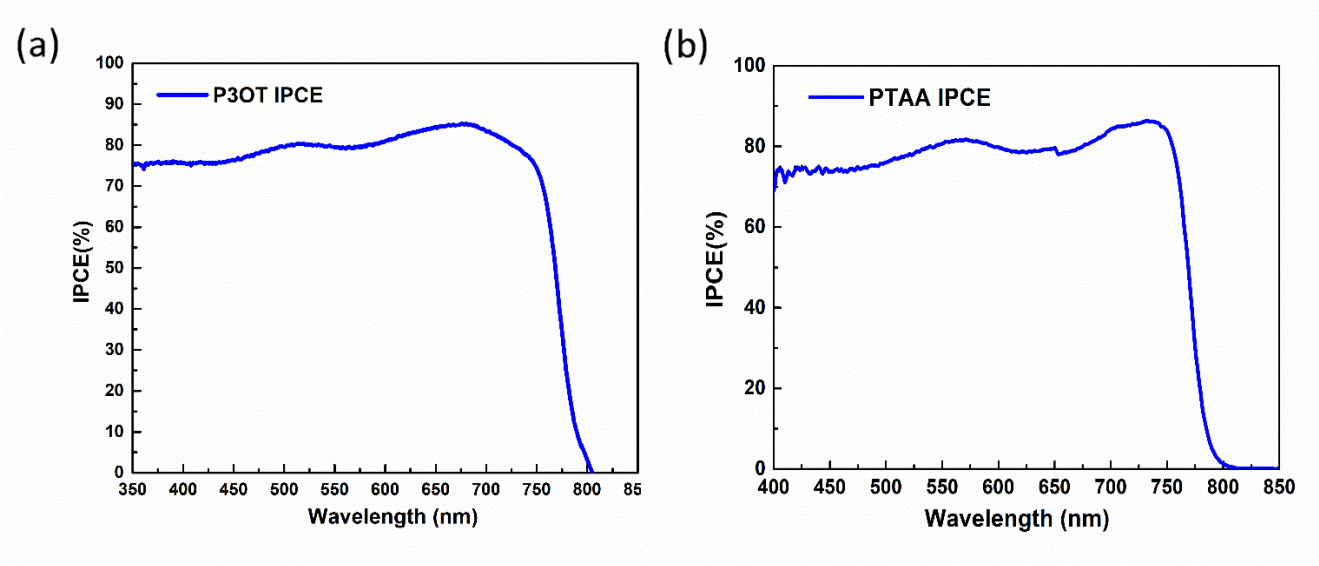

Supplementary Figure S8. *Incident Photon to Electron Conversion Efficiency (IPCE) spectra of the plasma treated P3OT (a) and PTAA (b) interlayer $CH_3NH_3PbI_3$ perovskite devices.*